



e-ISSN: 2278-8875
p-ISSN: 2320-3765

International Journal of Advanced Research

in Electrical, Electronics and Instrumentation Engineering

Volume 13, Issue 5, May 2024

ISSN INTERNATIONAL
STANDARD
SERIAL
NUMBER
INDIA

Impact Factor: 8.317

9940 572 462

6381 907 438

ijareeie@gmail.com

www.ijareeie.com



Capacitor Clamped LLC Resonant Converter for High Density EV Charger with a Lead-In to V2G Technology

Jerrin John Parakkal, Swapna K K

M. Tech Student (Power Electronics), Dept. of EEE, School of Engineering, Cochin University of Science and Technology, Kerala, India

Project Officer (Lecturer), Dept. of Technical Education, State Institute of Technical Teachers' Training and Research, Kerala, India

ABSTRACT: This paper presents a Capacitor-Clamped LLC resonant converter designed for high-power-density electric vehicle (EV) charging applications with future integration into Vehicle-to-Grid (V2G) systems. The proposed topology operates in the capacitive region, enabling high-frequency soft-switching to reduce switching losses and improve efficiency. The capacitor-clamped configuration enhances voltage regulation, reduces component stress, and supports a more compact and thermally efficient design. Featuring bidirectional power flow, the converter facilitates V2G capability, enabling energy exchange between EVs and the grid. A closed-loop control strategy ensures precise output voltage and current regulation under varying load conditions. Simulation results confirm the converter's high efficiency, minimal ripple, and strong dynamic performance. The proposed system offers a compact, reliable solution for next-generation smart EV charging infrastructure.

KEYWORDS: Capacitor-Clamped LLC, Bidirectional Converter, V2G, High-Power-Density Charger, Closed-Loop Control

I. INTRODUCTION

Recently, due to the energy shortage and environmental concerns of fossil fuel technologies, electric vehicles are gaining increasing popularity in the transportation sector. One of the key challenges of electric vehicle design is the development of high-performance charging technology. In addition to high-efficiency and low-cost, high-power density is equally important to charging system design. As the sizes of active components and their associated cooling systems in modern power electronics systems are getting increasingly smaller (due to the rise of new semiconductor technologies such as wide bandgap), the relative importance of the sizes of passive components, especially the magnetic, has dramatically increased. The rapid growth of electric vehicles (EVs) has led to an increased demand for efficient and high-power-density charging solutions. Traditional charging methods, such as using a diode bridge rectifier followed by a DC-DC converter, have limitations in terms of efficiency, size, and power density. Resonant converters, on the other hand, offer advantages in terms of higher efficiency, reduced size, and improved power density. The motivation behind this project is to design and implement a high-power-density EV charger using a Capacitor-Clamped LLC (C-LLC) resonant converter operating in the capacitive region. The C-LLC resonant converter has been recognized as a promising topology for high-power applications due to its ability to achieve high efficiency, compact size, and improved power density. By operating in the capacitive region, the converter can achieve high-frequency operation and further enhance its performance characteristics.

II. PROPOSED LLC RESONANT CONVERTER

In the quest for efficient and flexible power conversion systems, the capacitor clamped LLC resonant converter stands out due to its high efficiency and effective performance in various load conditions. This project focuses on modifying the traditional LLC resonant converter to enable bi-directional power flow and integrating a closed-loop current control mechanism. The LLC resonant converter is widely recognized for its soft-switching capabilities, which significantly reduce switching losses and electromagnetic interference. By incorporating a capacitor clamping technique, this converter enhances voltage regulation and reduces voltage stress on the components, leading to improved reliability and efficiency. The traditional LLC resonant converter primarily supports unidirectional power flow, which is suitable for standard



power supply applications. However, for applications like electric vehicle (EV) charging and renewable energy systems, bi-directional power flow is essential. Modifying the LLC resonant converter to be bi-directional allows it to not only charge batteries but also to return energy back to the grid or other sources, supporting functionalities such as vehicle-to-grid (V2G) and grid energy storage. To ensure precise control over the power conversion process, a closed-loop current control mechanism is integrated into the bi-directional LLC resonant converter. This control method continuously monitors the output current and adjusts the converter's operation to maintain the desired current levels. The benefits of closed-loop current control include improved stability, enhanced response to load variations, and better protection against overcurrent conditions. The key objectives of this project are: 1. To modify the traditional capacitor clamped LLC resonant converter for bi-directional power flow. 2. To implement a closed-loop current control system to enhance the accuracy and stability of the converter. 3. To evaluate the performance of the modified converter in terms of efficiency, reliability, and operational flexibility. The development of a capacitor clamped LLC resonant converter with bi-directional capabilities and closed-loop current control represents a significant advancement in power conversion technology.

CIRCUIT DIAGRAM AND CIRCUIT TOPOLOGY

The presented capacitor-clamped LLC resonant converter based on the half-bridge configuration is shown in Fig. 1. It comprises a half-bridge switch network formed by Q1 and Q2, a resonant network formed by a resonant inductor Lr, a pair of resonant capacitors C1 and C2 and a magnetizing inductor Lm of the transformer Tx (having a turn ratio of $n=N_p/N_s$: N_s , where N_p and N_s are the number of turns on the primary and secondary side of Tx, respectively), two clamping diodes D1 and D2 in parallel with C1 and C2, a full-bridge diode rectifier Do1 – Do4, and an output capacitor Co connected to the load. The control structure of the presented converter during CC mode of charging is shown. Here a Proportional- Integrator (PI) compensator is used for voltage regulation. This is possible as Vo is proportional to fixed switching frequency fsw. When Vo reaches a preset boundary value between the CC and CV mode, PI controller will be deactivated and fsw will be fixed to fo as Vo is constant during CV mode.

OPERATING PRINCIPLES

To simplify the analysis, it is assumed that, (i) Co is sufficiently large such that the output voltage Vo is constant (ii) the system is lossless with a conversion efficiency of 100%. The operation of the capacitor-clamped LLC resonant converter in capacitive region involves four possible modes of operation (Mode I – IV), of which the equivalent circuits are shown in Fig. 3, respectively, for the positive half switching cycle. Fig. 4 further illustrates the typical operating waveforms during steady-state operation. Due to symmetry of operation, only the positive half cycle of a switching period is analyzed. Before Mode I begins, the resonant inductor current $i_{Lr} < 0$ which ensures that Q1 can achieve ZVS. When i_{Lr} increases to zero, Mode I begins.

Mode I ($t_1 \leq t \leq t_2$): Mode I begins with $i_{Lr}(t_1) = 0$, and Q1 is turn on with ZVS. In Mode I, Do1 and Do4 are conducting, and thus the secondary voltage of Tx is Vo, and Lm is linearly charged by nVo.

Mode II ($t_2 \leq t \leq t_3$): In Mode II, Do1 and Do4 continue to conduct, and thus Lm is still charged by nVo. However, due to the presence of D1, Cr ceases resonating with Lr as D1 is forward biased by i_{Lr} . In particular, v_{C1} (v_{C2}) is constantly clamped to 0 (Vin) and Lr is linearly discharged by $-nVo$, i.e Mode II ends when $i_{Lr} = i_{Lm}$ and Do1 and Do4 are turned off at zero-current-switching (ZCS).

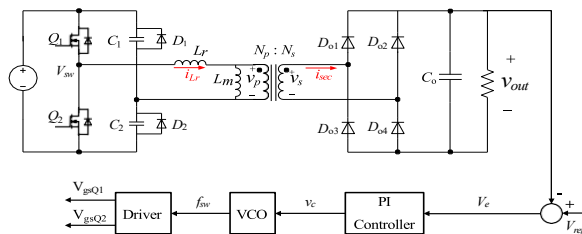


Fig. 1 Converter circuit

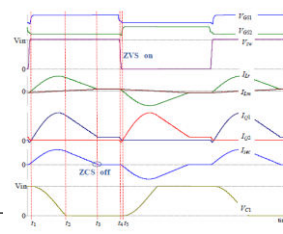


Fig. 2 Operating waveforms

Mode III ($t_3 \leq t \leq t_4$): In Mode III, Lr and Lm are connected in series and shorted by D1 and Q1. This means that i_{Lr} (i_{Lm}) and v_{C1} (v_{C2}) will remain constant during this mode. i.e., v_{C1} (v_{C2}) is 0 (Vin)

Mode IV ($t_4 \leq t \leq t_5$): At t_4 , Q1 is turned off. i_{Lr} will charge (discharge) the energy stored in the output capacitance Coss of Q1 (Q2). If sufficiently large, i_{Lr} will fully charge (discharge) the Coss of Q1 (Q2) and Q2 can be turned ON at ZVS.



During this mode, Do2 and Do3 are conducting, and thus L_m is linearly discharged by $-nV_o$, and L_r is linearly discharged by $(V_{in}-nV_o)$.

DESIGN AND DC CHARACTERISTIC OF CAPACITOR CLAMPED LLC RESONANT CONVERTER

Design case for EV charging application.

Assuming 100% power efficiency and according to energy conservation principle, we have: Notice that the input current is charging (discharging) C_2 (C_1) between V_{in} and 0 V during $t_1 - t_2$ in the positive (negative) half cycle while is zero for the rest of the positive (or negative) half cycle. Therefore, the average input current I_{in} over one switching cycle is: This means that the output power scales linearly with f_{sw} , and constant output power can be achieved at a fixed switching frequency f_{sw} . Unlike conventional LLC resonant converters that are operated in the ZVS region where the output power is a highly nonlinear function of the switching frequency, the presented resonant converter operated in the capacitive region follows a very simple linear relationship between f_{sw} and P_o . For EV charging, the system is initially charged at constant current (CC) mode, followed by constant voltage (CV) mode. In CC mode of charging, I_o is constant. Thus, V_o can be linearly regulated by controlling f_{sw} .

$$V_o = \frac{(C_1 + C_2)V_{in}^2 f_{sw}}{I_o}$$

As V_o (and thus P_o) increases, f_{sw} increases linearly. The endpoint of CC mode is the starting point of CV mode. Considering that P_o (and thus f_{sw}) varies significantly during CV mode of operation while V_o is constant, the capacitor-clamped LLC converter may be designed such that the full output power precisely corresponds to the optimal operating point of an LLC resonant converter. This is the point where (i) the converter is just about to leave the capacitive mode while entering the inductive mode, and (ii) the voltage gain of the converter is constant. The key advantages of operating the converter back in the inductive mode and at the resonant frequency during the CV mode of operation are to achieve (i) ideally zero frequency variation during CV mode and (ii) maximum efficiency at full output power. Correspondingly, the resonant capacitance can be selected as

$$C_1 = C_2 = \frac{P_{o\max}}{2V_{in}^2 f_o}$$

The minimum operation frequency happens at the start point of CC mode when V_o and P_o is minimum:

$$f_{o\min} = \frac{V_{o\min}}{V_{o\max}} f_o$$

III. SIMULATION AND RESULTS

The capacitor-clamped LLC resonant converter offers a high-efficiency power conversion solution with inherent soft-switching characteristics that minimize switching losses and electromagnetic interference. This project introduces modifications to the conventional LLC converter, enabling bidirectional power flow and integrating a closed-loop current control system for enhanced performance. The bidirectional operation is critical for Vehicle-to-Grid (V2G) applications, allowing energy transfer from the grid to the vehicle and vice versa. The capacitor clamp improves voltage regulation and reduces stress on circuit components, contributing to better efficiency and long-term reliability. A closed-loop control mechanism is employed to monitor output current in real-time, dynamically adjusting system parameters to maintain stability and protect against overcurrent events. MATLAB simulations validate the converter's performance under varying load conditions. Key findings include consistent high efficiency, stable current regulation, and successful bidirectional operation—demonstrating the converter's potential for future-ready EV charging and smart energy systems.

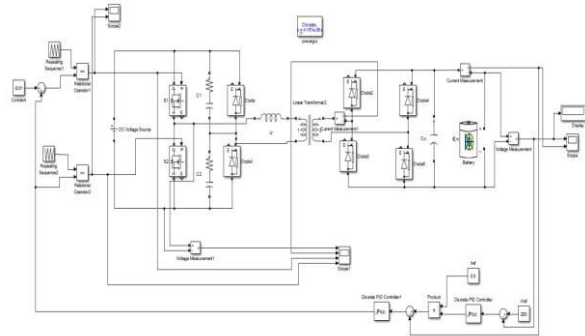


Fig 3 Simulink model of original circuit with current

MATLAB/SIMULINK MODEL & SIMULATIONS

The output of the converter shows that when the output voltage is restricted to 200V the value of the output current decreases and is equal to .8A. There is decrease in output current when output voltage increases. When the output is less than 200V i.e around 140V the output current increases and is around 2.7A so that there is no control in the charging current. The output of the converter when current feedback is added to the circuit shows that when the output voltage is restricted to 200V the value of the output current is also limited to the set value equal to 1.6A. Hence the output current can be controlled by introducing a current loop into the original circuit. There are no large variations in the current and a current limiting switch can be avoided.

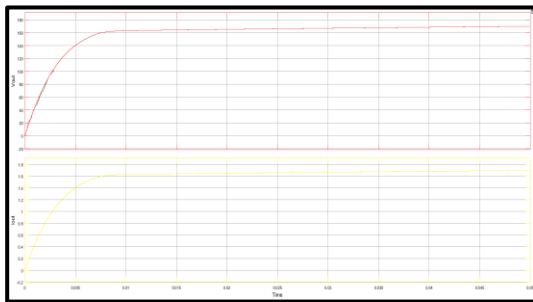


Fig.3 Output current when voltage of 200V required to charge battery

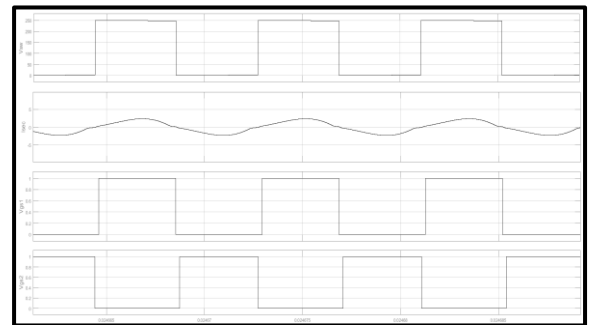


Fig.4 ZVS and ZCS for the simulated converter

IV. DESIGN AND IMPLEMENTATION OF HARDWARE PROTOTYPE

This project focuses on the design and development of a **hardware prototype** of a **bidirectional LLC resonant converter-based EV charger**, supported by a **miniature scale model** and an **IoT-enabled graphical user interface (GUI)** for enhanced control and monitoring. The bidirectional LLC topology is selected for its high efficiency, low electromagnetic interference, and adaptability to varying load conditions—key attributes for modern **EV charging and Vehicle-to-Grid (V2G)** systems. The converter allows power transfer both to and from the grid, enabling EVs to function as distributed energy storage units. A scaled-down physical model will replicate the key components, including power circuits and control systems, to illustrate real-time operation. An **IoT-integrated GUI** will provide users with remote access to charging data, power flow status, and system diagnostics. This interface enhances usability and system visibility. Project goals include building the prototype, developing the scale model, implementing the GUI, and evaluating system efficiency and user experience.

HARDWARE PROTOTYPE DESIGN AND IMPLEMENTATION

From the equations 1 to 18 given above the values of the circuit parameters were calculated and as shown in the table given below. The system is designed for 24V input voltage (V_{in}) and an output power (P_o) of 30W. The output voltage can be varied from 15V to 30V. The resonant frequency is taken as 120KHz. The designed parameters of prototype are as given below: Input voltage , $V_{in} = 24V$. Output voltage, $V_o = 15V$ to 30 V range, Resonant frequency $f_o = 120kHz$. Resonant capacitors, $C_1 = C_2 = 0.2 \mu F$ Resonant inductor $L_r = 4.4 \mu H$ neglected as the inductance is too small



and can be catered by the transformer windings. Transformer turns ratio = $n = 0.5$ But taken as 1 by trial-and-error method for making the circuit bidirectional. Frequency min, $f_{min} = 60\text{kHz} = 60\text{kHz}$



Fig.5 Prototype setup

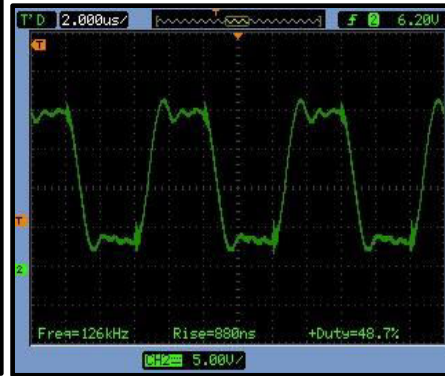


Fig.6 Resonant capacitor voltage

To testify the characteristics and evaluate the current control of the presented converter a prototype setup of the bidirectional charger is constructed with the same circuit parameters. The experimental prototype of the presented converter is shown in the waveform in Fig. 6 shows the resonant capacitor voltage during the switching cycle of the presented converter. The resonant capacitor voltage switches with the switching signals in ZVS mode. The capacitor voltage is identical in both directions and is symmetrical and hence the average value of the voltage is 0. This indicates that the loss in the circuit is minimum. Also switching losses can be minimized by making the circuit work in resonant frequency of 120kHz. Plot 1 is the volage across the switch during the operation and plot 2 is the switching signals in the second MOSFET. This indicates that switching of the circuit takes place during the ZVS as the switching takes in the zero point of the voltage. The same plot can be plotted with the other symmetrical switch which also shows a similar characteristic but in the opposite direction.

Experimental results and output characteristics.

The performance of the proposed converter was evaluated under both open-loop and closed-loop current control configurations, with the operating frequency varied from 60 kHz up to and beyond the resonant frequency of 120 kHz. A 24V lead-acid rechargeable battery was used as the load for testing. Output voltage and charging current values were recorded across different frequencies and are summarized in Tables 1 and 2 for open-loop and closed-loop cases, respectively. In the open-loop mode, the output voltage rises with increasing frequency and reaches its peak at the resonant point. During this phase, the system operates in Constant Current (CC) mode, where both voltage and current increase. Beyond the resonant frequency, the output voltage stabilizes while the current continues to increase in an uncontrolled manner, transitioning into Constant Voltage (CV) mode. This behavior indicates a lack of current regulation beyond the resonance point in open-loop operation. Conversely, the closed-loop system, shown in Figure 25, exhibits improved control characteristics. With increasing frequency, the output voltage reaches a maximum at resonance, similar to the open-loop case. However, the output current remains stable, effectively maintaining CC mode. After the resonant frequency, while the voltage remains constant, the current decreases slightly and stabilizes as the battery approaches full charge, representing a well-controlled CV mode.

Figure 8 illustrates the input-output power characteristics of the closed-loop system. It shows that the input power remains nearly constant, while the maximum output power is attained precisely at the resonant frequency, indicating optimal operation. In contrast, the open-loop system reaches peak power at frequencies above resonance. Overall, the closed-loop system demonstrates superior efficiency, improved current control, and reduced power consumption for the same output, as confirmed by the efficiency curves in the accompanying figures.



Sl no.	Frequency	Output Voltage V	Output Current I	Input Voltage V	Input Current I	Efficiency %
1	60	18.930	0.890	30.36	1.8	30.83
2	65	19.250	0.900	30.36	1.8	31.70
3	70	19.590	0.928	30.36	1.8	33.27
4	75	19.970	0.940	30.36	1.8	34.35
5	80	20.270	0.960	30.36	1.8	35.61
6	85	20.580	0.970	30.36	1.8	36.53
7	90	20.900	0.990	30.36	1.8	37.86
8	95	21.330	1.000	30.36	1.8	39.03
9	100	21.740	1.032	30.36	1.8	41.05
10	105	22.380	1.064	30.36	1.8	43.57
11	110	22.690	1.080	30.36	1.8	44.84
12	115	23.170	1.111	30.36	1.8	47.10
13	120	23.190	1.120	30.36	1.8	47.53
14	125	23.192	1.230	30.36	1.8	52.20
15	130	23.200	1.380	30.36	1.8	58.59

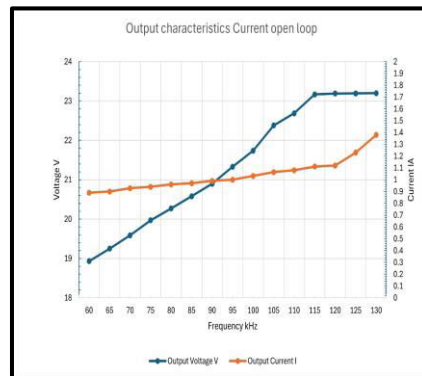


Table 1: Input and output values of voltage and current in open loop circuit without current control

Fig. 7 Output characteristics open loop circuit

In a closed loop system, the maximum efficiency occurs at the resonant frequency and the output current can be controlled within the limits and maximum power can be transferred to the output. In an open loop the charging current cannot be controlled and goes on rising after the resonant frequency. The current can be limited only by the current limiter switch in this converter. Maximum power transfer takes place in a frequency greater than resonant frequency and the system is getting uncontrollable.

Sl No.	Frequency (kHz)	Output Voltage V	Output Current I (A)	Input Voltage V	Input Current I(A)	Efficiency %
1	60	20.20	0.79	30.36	0.754	69.71
2	65	21.30	0.79	30.36	0.754	73.51
3	70	22.00	0.79	30.36	0.754	75.92
4	75	22.60	0.79	30.36	0.754	77.99
5	80	23.30	0.79	30.36	0.754	80.41
6	85	24.20	0.79	30.36	0.754	83.52
7	90	25.00	0.79	30.36	0.754	86.28
9	95	25.60	0.79	30.36	0.754	88.35
10	100	26.20	0.79	30.36	0.754	90.42
11	105	26.65	0.79	30.36	0.754	91.97
12	110	27.00	0.79	30.36	0.754	93.18
13	115	27.50	0.79	30.36	0.754	94.90
14	120	27.99	0.79	30.36	0.754	96.60
15	125	28.20	0.75	30.36	0.754	92.39
16	130	28.20	0.75	30.36	0.754	92.39
17	135	28.20	0.75	30.36	0.754	92.39

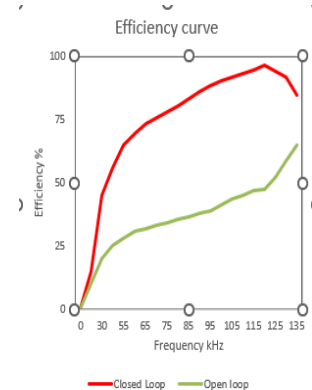
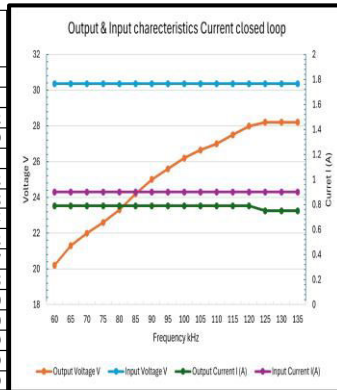


Table 2 Input and output values of voltage

Fig. 8 Output & Input chara

Fig. 9 Efficiency curve and current in closed loop circuit with current control

V.CONCLUSION AND FUTURE SCOPE

This paper reports my investigation into the operation of a capacitor-clamped LLC resonant converter for high density EV chargers with a lead-in to the V2G technology. The presented converter was designed for a bidirectional resonant converter which showed similar characteristics base converter [1]. The frequency- voltage relationship of the converter as per the design was verified. The ZVS and ZCS were verified for the presented converter. The bidirectionality feature of the presented converter was studied and it has shown the same characteristics in both directions. The current control loop into the base converter has made the presented converter more current controllable and helped the converter to deliver maximum power at the resonant frequency. This also eliminated the use of current limiter switch in the conventional EV charger and made the circuit current controllable. The efficiency of the system at resonant frequency has improved and the system delivers maximum power at maximum efficiency. The miniature still models of solar carport for long term parking with smart EV chargers unlatched the possibility of incorporating V2G technology to the transportation and service sector like CIAL for unfolding novel ideas for the futuristic planning and management of renewable energy and grid stabilization. The development of IOT based software and mobile application and incorporating it to the charger has made the charger smarter and lead-in to an economic model for the EV owners to make an income and add to the grid support by reducing the cost and space of the large battery energy storage system BEMS and thereby making the system smarter, greener, and healthier. The combined effect of these new features may lead to simultaneously high efficiency, power density, and low-cost design, essential to EV charging applications which shall be



grid communicating to facilitate V2G technology. Both simulations and experiments have been conducted to verify these new features of the converter. Future works may include a thorough design optimization and characterization of the proposed concept. The major limitation of the half-bridge structure is its lower power ratings as compared to full-bridge ones. In future work, will investigate the following two possible solutions to higher power applications: 1) Connecting several half-bridges 2) Extend the idea to full bridge converters. 3) Develop an IOT based software specific for the EV charging with integration of different databases of Airport, Power grid and Electric vehicle. 4) Implement the project as a pilot plant in the airport after studying and researching all possible means for reducing the cost, size, and interface magnetics of the EV chargers.

REFERENCES

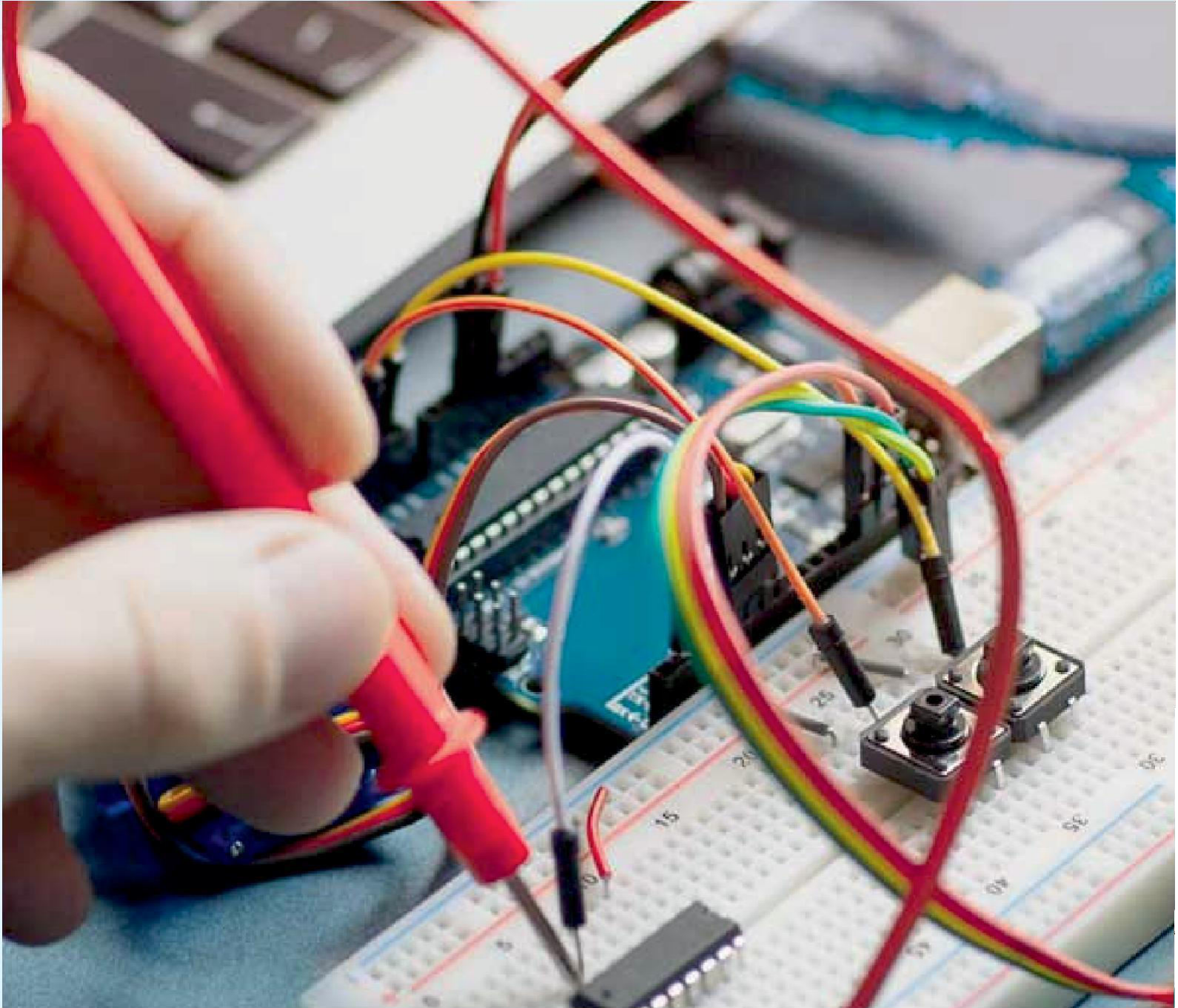
- [1] Capacitor clamped LLC Resonant Converter Operating in Capacitive -Region for High power density EV charger by Jiayang Wu, AinanLi, Siew-Chong Tan , IEEE transactions on Power electronics
- [2] C. C. Chan, "The State of the Art of Electric, Hybrid, and Fuel Cell Vehicles," Proceedings of the IEEE, vol. 95, no. 4, pp. 704-718, April 2007
- [3] M. Yilmaz and P. T. Krein, "Review of Battery Charger Topologies, Charging Power Levels, and Infrastructure for Plug-In Electric and Hybrid Vehicles," IEEE Transactions on Power Electronics, vol. 28, no. 5, pp. 2151-2169, May 2013
- [4] H. Hu, X. Fang, F. Chen, Z. J. Shen, I. Batarseh, "A modified high- efficiency LLC converter with two transformers for wide input-voltage range applications," IEEE Trans. Power Electron., vol. 28, no. 4, pp. 1946-1960, Apr. 2013.
- [5] I. H. Cho, Y. D. Kim, and G.W.Moon, "A half-bridge LLC resonant converter adopting boost PWM control scheme for hold-up state operation," IEEE Trans. Power Electron., vol. 29, no. 2, pp. 841–850, Feb. 2014.
- [6] B. Li, Q. Li, F. C. Lee, Z. Liu, and Y. Yang, "A High-Efficiency High- Density Wide-Bandgap Device-Based Bidirectional On-Board Charger," IEEE Journal of Emerging and Selected Topics in Power Electronics, vol. 6, no. 3, pp. 1627-1636, 2018.
- [7] H. Wu, Y. Li, and Y. Xing, "LLC Resonant Converter with Semiactive Variable-Structure Rectifier (SA-VSR) for Wide Output Voltage Range Application," IEEE Trans. Power Electron., vol. 31, no. 5, pp. 3389– 3394, May. 2016.
- [8] G. Liu, Y. Jang, M. M. Jovanovi, and J. Q. Zhang, "Implementation of a 3.3-kW DC–DC Converter for EV On-Board Charger Employing the Series-Resonant Converter With Reduced-Frequency-Range Control," IEEE Transactions on Power Electronics, vol. 32, no. 6, pp. 4168-4184, 2017.
- [9] H. Wang, M. Shang, and D. Shu, "Design Considerations of Efficiency Enhanced LLC PEV Charger Using Reconfigurable Transformer," IEEE Trans. Veh. Technol., vol. 68, no. 9, pp. 8642–8651, Sep. 2019.
- [10] H. Wang and Z. Li, "A PWM LLC Type Resonant Converter Adapted to Wide Output Range in PEV Charging Applications," IEEE Transactions on Power Electronics, vol. 33, no. 5, pp. 3791-3801, May 2018.
- [11] H. Haga and F. Kurokawa, "Modulation Method of a Full-Bridge Three- Level LLC Resonant Converter for Battery Charger of Electrical Vehicles," IEEE Transactions on Power Electronics, vol. 32, no. 4, pp. 2498-2507, April 2017."
- [12] M. Noah et al., "Magnetic Design and Experimental Evaluation of a Commercially Available Single Integrated Transformer in Three-Phase LLC Resonant Converter," IEEE Transactions on Industry Applications, vol. 54, no. 6, pp. 6190-6204, Nov.-Dec. 2018.
- [13] C. Fei, F. C. Lee and Q. Li, "High-Efficiency High-Power-Density LLC Converter With an Integrated Planar Matrix Transformer for High- Output Current Applications," IEEE Transactions on Industrial Electronics, vol. 64, no. 11, pp. 9072-9082, Nov. 2017.
- [14] D. Junjun, L. Siqu, H. Sideng, C. C. Mi, and M. Ruiqing, "Design Methodology of LLC Resonant Converters for Electric Vehicle Battery Chargers," IEEE Transactions on Vehicular Technology, vol. 63, no. 4, pp. 1581-1592, 2014.
- [15] F. Musavi, M. Craciun, D. S. Gautam, W. Eberle, and W. G. Dunford, "An LLC Resonant DC–DC Converter for Wide Output Voltage Range Battery Charging Applications," IEEE Transactions on Power Electronics, vol. 28, no. 12, pp. 5437-5445, 2013.
- [16] R. W. Erickson and D. Maksimovic, Fundamentals of Power Electronics, MA, Norwell:Kluwer, 2001.
H. Choi, "Half-Bridge LLC Resonant Converter Design Using FSFR- Series Fairchild Power Switch", Fairchild Semiconductors, AN-4151.
- [17] B. Lu, W. Liu, Y. Liang, F. C. Lee, J. D. van Wyk, "Optimal design methodology for LLC resonant converter", Proc. IEEE Appl. Power Electron. Conf., pp. 533-538, 2006.
- [18] R. Yu, G. K. Y. Ho, B. M. H. Pong, B. W.-K. Ling, and J. Lam, "Computer-Aided Design and Optimization of High-Efficiency LLC Series Resonant Converter," IEEE Transactions on Power Electronics, vol. 27, no. 7, pp. 3243-3256, 2012.
- [19] Z. Hu, L. Wang, H. Wang, Y. Liu and P. C. Sen, "An Accurate Design Algorithm for LLC Resonant Converters— Part I," IEEE Transactions on Power Electronics, vol. 31, no. 8, pp. 5435-5447, Aug. 2016.



|| Volume 13, Issue 5, May 2024 ||

| DOI:10.15662/IJAREEIE.2024.1305067 |

- [20] Z. Hu, L. Wang, Y. Qiu, Y. Liu and P. C. Sen, “An Accurate Design Algorithm for LLC Resonant Converters—Part II,” IEEE Transactions on Power Electronics, vol. 31, no. 8, pp. 5448-5460, Aug. 2016.
- [21] P. Foster, and D. A. Stone, “Describing function model of series resonant inverter with current limiting diode-clamp,” Electronics Letters, vol. 47, no. 25, pp. 1363-1364, 2011.
- [22] C. W. Tsang, M. P. Foster, D. A. Stone, and D. T. Gladwin, “Analysis and Design of LLC Resonant Converters With Capacitor–Diode Clamp Current Limiting,” IEEE Transactions on Power Electronics, vol. 30, no. 3, pp. 1345-1355, 2015.



INNO  SPACE
SJIF Scientific Journal Impact Factor

 **doi**[®]
cross **ref**

 **INTERNATIONAL
STANDARD
SERIAL
NUMBER
INDIA**



International Journal of Advanced Research

in Electrical, Electronics and Instrumentation Engineering

 9940 572 462  6381 907 438  ijareeie@gmail.com



www.ijareeie.com

Scan to save the contact details